DOI: 10.1002/asia.200600009

Using Bioconjugated Nanoparticles To Monitor *E. coli* in a Flow Channel

Shelly John Mechery, Xiaojun Julia Zhao, Lin Wang, Lisa R. Hilliard, Alina Munteanu, and Weihong Tan*[a]

Abstract: A simple and portable flow channel optical detection system combined with bioconjugated luminescent nanoparticles allows the rapid detection of single bacterial cells without sample enrichment. The optical system is designed to have single-molecule-detection capability in a microcapillary flow channel by decreasing the laser excitation probe volume to a few picoliters, which consequently results in a low background. Specific monoclonal antibodies were immobilized on nanoparticles to form nanoparticle–antibody conjugates. The bioconjugated nanoparticles bind to the target bacteria when they recognize the antigen on the bacterium surface, thus providing a bright luminescent signal for the detection of individual bacteria cells. The high sensitivity provided by the luminescent and photostable silica nanoparticles eliminates the need for further enrichment of bacteria samples and signal amplification. This flow channel detection system is convenient and allows the detection of single bacterial cells within a few minutes.

Keywords: antibodies · biosensors · luminescence · nanostructures

Introduction

The rapid and accurate detection of trace amounts of pathogenic bacteria is important in food safety, clinical diagnosis, and military/civilian warfare. Recently, there has been much interest in the detection and identification of various microorganisms owing to the increased risks of terrorism with biological warfare agents. *Escherichia coli* O157:H7 (*E. coli* O157:H7) is one of the most dangerous food-borne pathogenic bacteria.[1] It can be found in raw beef, fruits, vegetables, salad-bar foods, salami, and other food products.[2,3] Outbreaks of *E. coli* O157:H7 infections have caused serious illnesses and led to a significant number of deaths.[2] Therefore, to prevent any accidental outbreaks or intentional terrorist acts, early detection of trace amounts of *E. coli* O157:H7 as well as other pathogenic bacteria and endospores are critical.

[a] S. J. Mechery, X. J. Zhao, L. Wang, L. R. Hilliard, A. Munteanu, W. Tan
Center for Research at the Bio/Nano Interface
Department of Chemistry and the Shands Cancer Center
University of Florida
Gainesville, FL 32611 (USA)
Fax: (+1) 352-846-2410
E-mail: tan@chem.ufl.edu

Supporting information for this article is available on the WWW under http://www.chemasianj.org or from the author.

The key requirements for any technique for the early detection of bacteria are sensitivity, specificity, and speed.[4] Conventional detection methods provide relatively highly sensitive, qualitative, and quantitative information only in the presence of substantial quantities of bacteria species, typically ranging from 100–100 000 CFU mL^{-1} (CFU = colony-forming unit). However, time constraints and easy on-site or universal analysis are the major limitations, because many of these methods rely on the ability of microorganisms to grow into visible colonies over time in special growth media, and this growth may take 1–5 days. Over the past several years, attempts have been made to improve traditional bacteria-detection methods through modification and automation, mainly focusing on decreasing the overall assay time. In addition, many developments in this direction are based on advances in analytical-based detection techniques, such as the direct epiluminescent filter technique (DEFT), mass-spectrometry-based methods, and counting and identification test kits.[5–10] One of the most promising techniques is flow cytometry,[11] which allows the detection of 10^2–10^3 *E. coli* O157:H7 cells/mL within 1 h on the basis of a luminescence signal in a flow system.[8,12] Even though the detection time is dramatically shortened, improved sensitivity is still a major challenge.

To improve the sensitivity and to reduce the detection time required for accurate bacteria detection further, a simple and inexpensive fluorescence-based detection system was developed. In this case, the optical system was designed

to have single-molecule-detection capability by reducing the laser probing volume to few a picoliters in the channel. Luminescent and bioconjugated silica nanoparticles were used to increase the analytical sensitivity of this system.[13,14] Recently, nanomaterials have been used in bioanalytical applications and show great promise.[13–20] Among the many different types of nanomaterials for bioanalysis, we have developed luminophore-doped silica nanoparticles (NPs) for a variety of interesting biotechnological applications.[13,14] These NPs have some unique features such as an intense luminescent signal, excellent photostability, and easy bioconjugation for linkage between nanomaterials and biological molecules for biological interactions and recognition. In addition, these NPs can be prepared easily and their surfaces can be modified with desired surface properties, such as charge and functionality. The signal enhancement of luminescent NPs is based on the tens of thousands of luminescent dye molecules contained in a single NP, which forms the foundation for luminescence detection with significant optical-signal amplification. In the present strategy for bacteria analysis, the recognition of a binding site, (i.e., an antibody–antigen interaction on a bacteria surface) is signaled by a nanoparticle conjugated to the antibody instead of a dye molecule. Thus, the luminescent signals are tens of thousands times stronger than that provided by a single dye,[14] providing highly amplified signals for single bacterium samples given the fact that many nanoparticles interact with a single bacteria cell. The NPs were treated by immobilizing monoclonal antibodies that specifically bind to *E. coli* O157:H7 surface antigen for the recognition of the specific bacteria. A prototype flow cytometer (Figure 1) and nanoparticle–antibody conjugates were designed for easy manipulation and portability and tested for potential field applications. Herein, we show that bacteria cells attached to nanoparticle–antibody conjugates were accurately detected and counted by the flow-channel detection system with high sensitivity, speed, and excellent reproducibility.

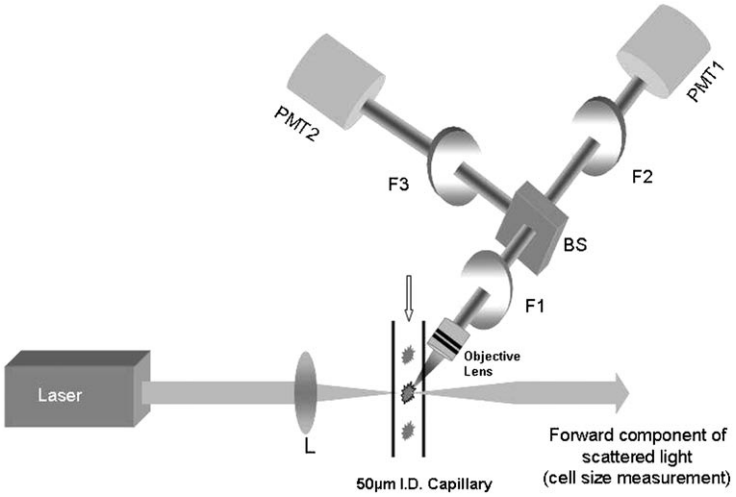

Figure 1. Schematic diagram of the luminescence flow cytometer. PMT-1 and PMT-2 are the photomultiplier tubes. F1, F2, F3 are long pass filters at 495 nm, 570 nm, and 650 nm respectively. Samples were pumped through the capillary with a syringe and a mechanical syringe-pump system.

Abstract in Chinese:

将流式通道光学检测系统与经过生物分子修饰的荧光纳米粒子相结合，我们建立了一种不经富集即可快速检测单个细菌的方法。该流式通道系统灵敏度高，可在几分钟内检测单个细菌，快速且操作方便。该系统通过降低流式通道中激光激发探针体积至几皮升，而降低检测背景，达到检测单个细菌的能力。纳米粒子与特异性单抗结合而成的复合物能特异性识别细菌表面的抗原并结合到其表面。由于单个纳米粒子含有成千上万个荧光分子，因此单个细菌即可产生很强的荧光信号，且光稳定，不需要进行细菌的富集和信号放大。为验证该系统的准确性，我们将纳米粒子细菌计数法与培养皿计数法获得的细菌数量比较，两种方法所得结果能够很好地吻合。该细菌检测方法灵敏度高，操作简易，重复性好，并且在各种检测样品中显示良好的特异性。

Results and Discussion

Bioconjugated Luminescent Nanoparticles for Pathogenic Bacteria Recognition

Luminescent NPs with sizes of 60 ± 4 nm were prepared for this application (Figure 2a). Tens of thousands of dye molecules are encapsulated within each NP. For the recognition of bacteria, the monoclonal antibodies were immobilized on the NPs, thus making the conjugates highly selective for *E. coli* O157:H7 in the immunoassay-based detection. Therefore, the antibody-conjugated NPs associated specifically with *E. coli* O157:H7 cell surfaces only (Figure 2b), but not with *E. coli* Dh5α, which lacks the surface O157:H7 antigen (Figure 2c). The SEM image of the *E. coli* O157:H7 cell after incubation with the NPs shows that there are many nanoparticle–antibody conjugates bound to a single bacterial cell, providing significant luminescent signal amplification relative to the single-dye-molecule assay. The greatly amplified and photostable luminescent signals from NPs attached to the bacteria surface easily enabled us to distinguish the spikes of the bacteria from the background, even when only one bacterium existed in the sample. The luminescence intensity of one RuBpy-doped NP (RuBpy = tris(2,2′-bipyridyl)dichlororuthenium(II) hexahydrate) was equivalent to that of more than 10^4 RuBpy molecules.[14] When monoclonal antibodies were immobilized on the NPs for the immunoassay, results showed that the presence of the NPs did not decrease the affinity of the antibody for the antigen. In contrast, the affinity constants may have been slightly higher than the intrinsic affinity of the antibody.[21]

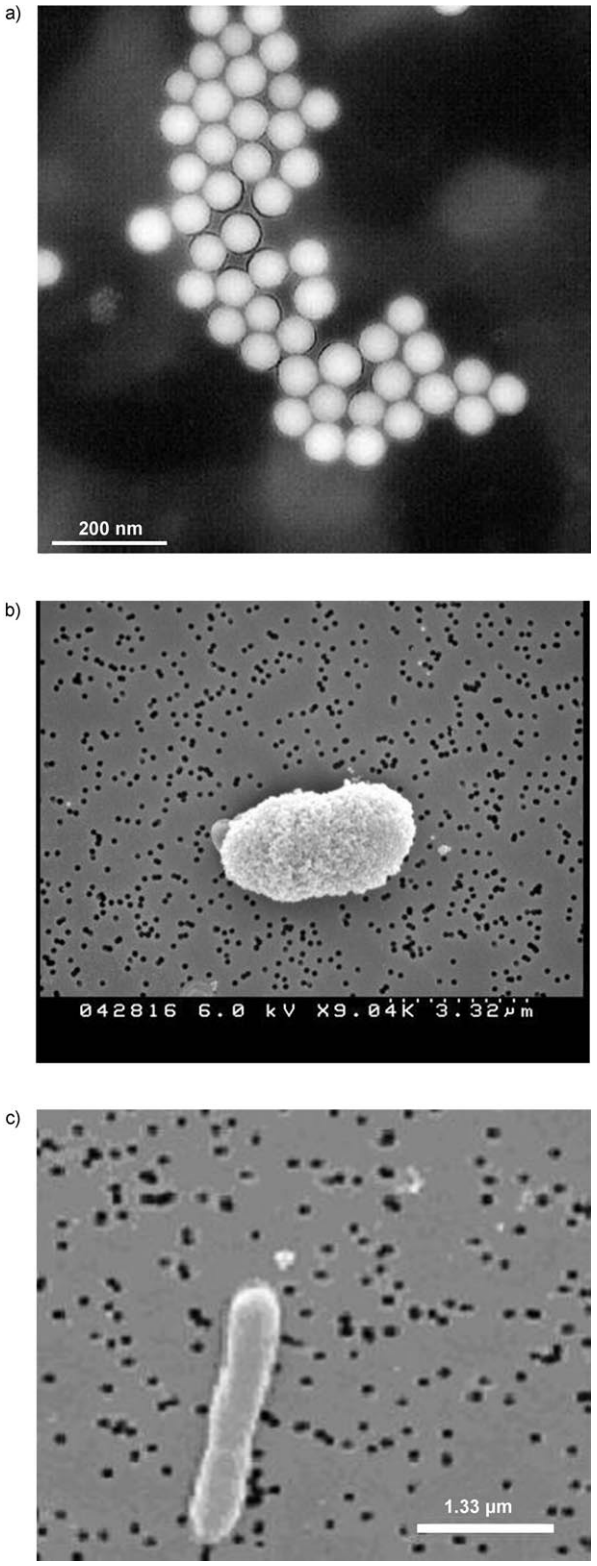

Figure 2. SEM images of immunological-based bacteria detection by using fluorescent dye-doped silica nanoparticles. a) Fluorescent-dye-doped silica nanoparticles ready for bioconjugation with antibodies for bacterial antigen recognition. b) *E. coli* O157:H7 bacteria cell with antigen-bound nanoparticle-O157–antibody conjugates. c) Negative-control bacteria, *E. coli* O157:Dh5α, with no antigen-bound nanoparticle-O157–antibody conjugates owing to the specificity of the antibody on the nanoparticle for *E. coli* O157:H7 only and not for other strains of *E. coli*.

The NP–antibody conjugates on the surface of the bacteria showed a strong binding affinity to *E. coli* O 157:H7 cells and thus gave very bright luminescent signals. The luminescence signals provided by the NPs are not only very bright but are also reproducible owing to the greatly decreased photobleaching by the silica matrix of the NPs.[13] This high photostability of the NPs provides reliable measurements, which are important for the detection of bacteria in more-practical settings. The NPs are thus unique in providing reproducible and highly amplified signals for the detection of bacteria as well as for other biorecognition needs.

Selection of Positive Signals from the Background in the Flow Channel System

The flow cytometry setup works well for counting bacteria. The strong fluorescence signal emitted and detected by a photomultiplier tube (PMT) during the passage of each bacterial cell through the probe volume represented a "detection event" in the analysis of the given sample. However, the recorded fluorescence data is an ensemble of positive spikes embedded in background noise. Figure 3a represents data recorded for a typical fluorescence burst during acquisition when bacteria–NP–antibody conjugates flow through the detection channel at a flow rate of $1\,mL\,h^{-1}$. To check the potential noise contribution in the background from additional noise sources like bacterial cell autofluorescence and PMT dark count, we have run plain bacterial samples prepared in PBS buffer (0.1 M) without attaching any probes (blank sample) through the flow channel. Figure 3b was recorded when the blank solution flowed through the sample cell. The threshold level, average signal intensity plus three times the standard deviation of the control sample (control-sample preparation is described in the Experimental Section) was set to discriminate the background noise from positive signals. Any fluorescence spike higher than the threshold level was treated as a positive signal and represented one bacterial cell. Therefore, counting the number of spikes above the threshold level was indicative of the exact amount of the target bacteria in the sample. Figures 3c and d show the fluorescence events above the threshold level of bacteria samples at concentrations of 5×10^5 and 1×10^5 cells mL^{-1}, respectively. Using this technique, we were able to detect one bacterial cell at a time. The sample flow rate and the sampling rates can be adjusted to meet the requirements of the different samples and analyses.

To evaluate the accuracy of this method in estimating bacterial counts, the average numbers of CFUs of *E. coli* O157:H7 in buffer (1 mL) were determined by plate counting. Various concentrations of freshly cultured homogenate *E. coli* O157:H7 were grown in growth media for approximately 24 h[22] and plated on plate-count agar; the colonies were then counted. These counts, the golden standard in microbiology,[22] were compared with the average numbers of *E. coli* O157:H7 detected by counting luminescent spikes from our flow-cytometry-based analysis. The results obtained by these two methods correlate well (Figure 4). Nota-

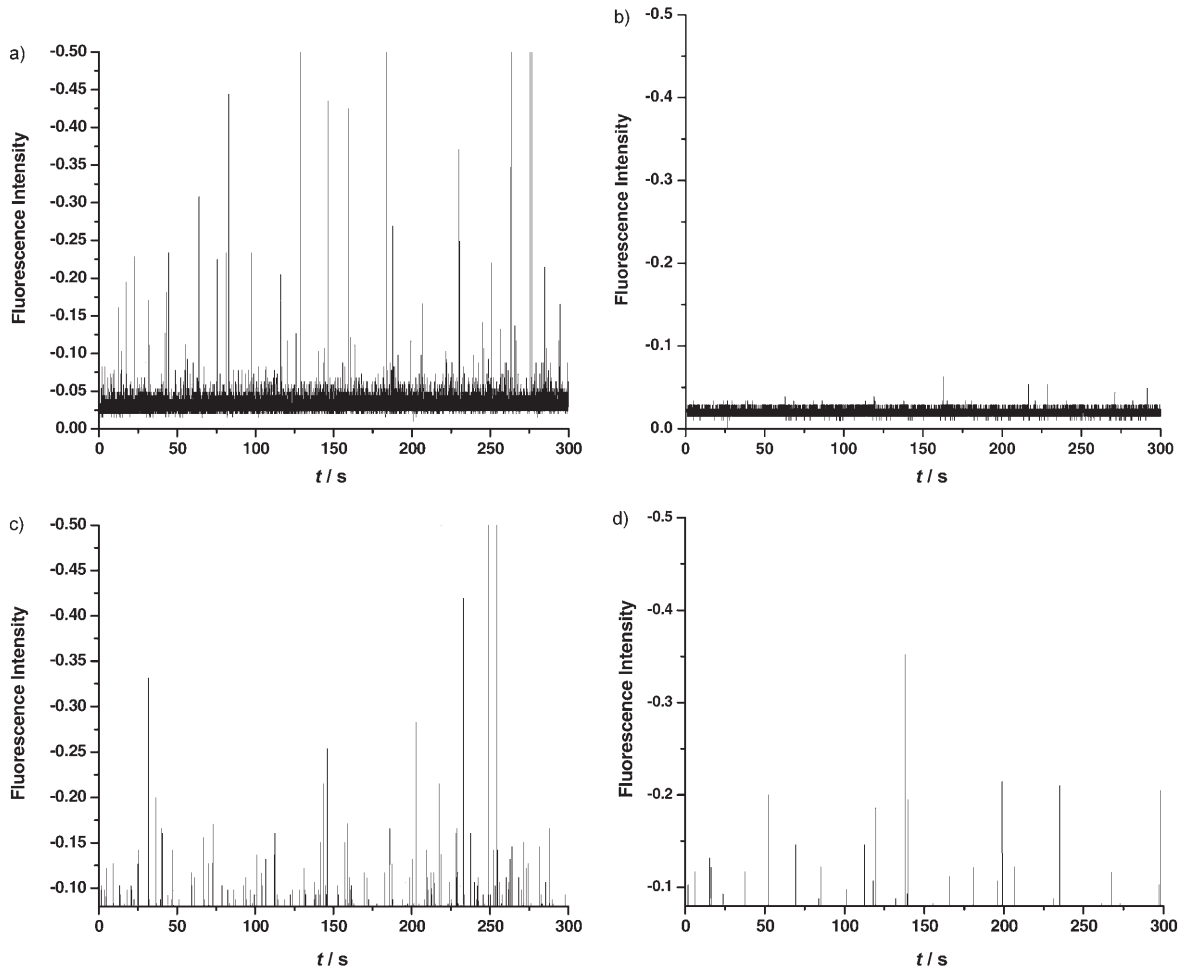

Figure 3. Typical flow-cytometry data for bacteria detection. a) Typical luminescence burst recorded during the data acquisition. b) Signals were recorded when a blank solution was flowed through the sample cell; c) and d) flow-cytometry trace at different concentrations of bacteria samples.

bly, it is not uncommon that the standard deviation in bacteria count when using the plate counting method is about 20 %.[12,22] This result clearly shows that the accuracy of our method is comparable to that of the plate counting method, but requires a much short time.

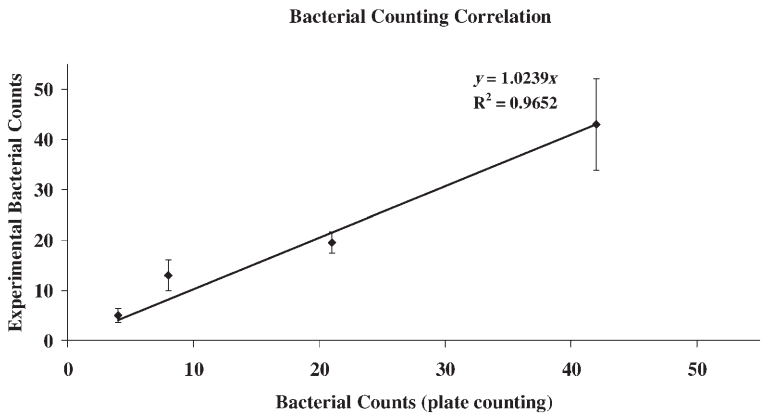

Figure 4. Comparison of flow-channel detection system with the "golden standard" for bacteria detection and counting. Number of *E. coli* O157:H7 cells detected by plating counting versus flow-cytometry counting. The data correlate well. The plate-counting method is the standard technique for bacterium counting.

Effect of the Probe Volume on the Sensitivity of the Flow Cytometry

To detect trace amounts of bacteria targets sensitively, it is critically important to decrease the background luminescence. The signal from a single-molecule dye or particle is independent of the probe volume, whereas the background signal is proportional to the probe volume. Hence, the background was minimized by using small probe volumes. Figure 5 shows the probe volume when a laser beam with Gaussian profile is used. Here, w_0 is the beam waist of the focused Gaussian beam in the capillary tube. The probe volume consists of two regions, with the central cylindrical region surrounded by a curved region.[23] The height of the cylinder in the present case is the

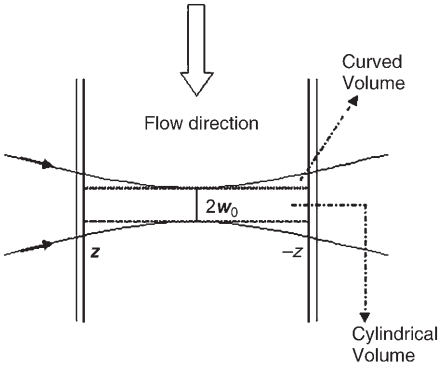

Figure 5. Schematic representation of the Gaussian probe volume containing cylindrical and curved volume contributions (w_0: laser beam waist, z: radius of the microcapillary).

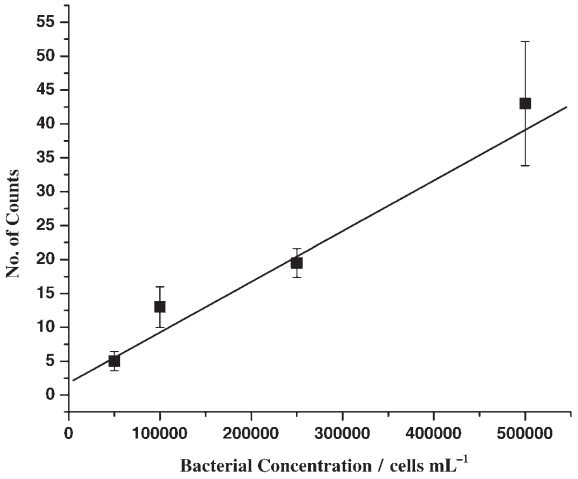

Figure 6. Calibration curve for the detection of bacteria cells by using the flow-channel detection system. Qualitative and quantitative information on samples comparable with current methods can be obtained by using this system. Given that the system is best utilized for trace analysis, it can also be used to analyze samples of 10^5 cells mL^{-1} and higher (data not shown for higher concentrations).

inner diameter of the capillary and the cylinder diameter is taken as the laser beam waist. A detailed calculation of the probe volume is provided in the Supporting Information. The probe volume could be decreased mainly by minimizing the capillary diameter of the flow channel. Thus, we used a diffraction limited achromatic lens with a focal length of 25 mm to focus the laser, which had a collimated beam diameter of 0.61 mm. The radius of the beam waist was calculated to be 9.6 μm. We have obtained a probe volume of 14 pL in the current flow-cytometer design. The present calculated probe volume is consistent with most of the single-molecule detection studies. The current optical-detection scheme ensures that the fluorescence-detection volume detected by the photomultiplier tubes is the same as the laser-probing volume. We tested the effect of different probe volumes on detectable luminescent signals for the same concentration of bacteria samples. The results showed that the smaller the probe volume, the better the signal-to-noise ratio.

Quantitative Determination of Bacteria Cells Based on Counting Luminescent Spikes

We counted several different concentrations of bacteria samples ranging from 5×10^4 to 5×10^5 cells mL^{-1} at a flow rate of 1 μL h^{-1}. The number of spikes in the flow-cytometry graph increased as the concentration of the bacteria sample increased. Figure 6 shows a calibration curve based on these results. To investigate the accuracy of the measurement further, we conducted false-positive and false-negative tests. Several blank samples were introduced into the detection system to determine if there is any false-positive signal. Then, several standard bacteria solutions of the same concentration were examined. Any failure to detect the presence of the targets would indicate a false-negative signal. The results showed that false-negative signals were insignificant and thus can be ignored. However, several false-positive signals were observed when the microchannel and sample cell were washed ineffectively. To minimize the false-positive signals, a washing solution containing NaOH (1 M) and tween 20 (1 %) was employed to clean the microcapillary until false-positive signals disappeared, before another round of analysis was conducted. The total sample analysis time from the sampling of the bacteria solution to the system analysis was less than 10 min. The flow rates were automatically controlled by the syringe-pump system, and thus the detection time was based upon the flow rate. The flow rates can be changed based on the bacteria concentration in the sample, and the sampling rates can be very high.

Uniformity of Burst-Size Distribution

We observed a nonuniform burst size distribution in the recorded luminescence data. Figure 3 reveals that intensities of the spikes are not uniform. These results are either due to nonuniform labeling of NPs on the bacteria surface or to the varied luminescence detection of bacteria species when it flows through the channel. Nonuniform labeling of bioconjugated nanoparticles to the biological samples is a major issue, especially in the burst-size distribution, which is being investigated further. The varied paths of the bacteria species as they transit the probe region is another source of the nonuniform luminescence spikes. Cells that diffuse exactly through the laser focus are excited with maximum efficiency and contribute an emission with large burst size, whereas cells that diffuse farther away from the laser focus are less excited with smaller burst size. More experiments with different excitation probe volume at various flow rates are being investigated further to confirm the contribution of the cell trajectories to the signal variability. Second, the rotation of the rod-shaped bacterial cells at different angles during the transit through the probe region and the consequent collection of the signals by the detector can cause a

variation of the signal. This problem was avoided in our analysis by conducting multiple experiments with both bacteria samples and control samples to set the right threshold in such a way as to minimize both false-negative and false-positive results. In our system, it seems that this strategy works well as the results shown in Figure 4 and from our control experiments both suggest that the determination of bacteria samples is accurate. The nonuniform spike size was thus not a major problem as long as the size of the spikes generated by the bacteria–NP conjugates is higher than the threshold. This is one important advantage of using NPs for this analysis as they provide strong signals upon binding to the surface of the bacteria.

Conclusions

We have developed a simple flow-channel detection system for rapid and sensitive analysis of bacteria cells. The system was combined with dye-doped silica NPs that provide high luminescent signal and can be easily used for bioconjugation with molecular probes for bioanalysis. The use of luminescent silica NPs not only provided significant signal amplification in bacteria antibody–antigen recognition, but also presented highly photostable luminescent signals for reproducible measurements. In less than 20 min, single *E. coli* O157:H7 bacteria cells can be determined with excellent reproducibility and specificity. The counting results correlate well with the standard plate counting method. Our method is rapid, technically simple, highly sensitive, and efficient. This assay can potentially be adapted for the detection of a wide variety of bacteria pathogens by using antibodies specific for various bacteria pathogens.

Experimental Section

Chemicals

Tetraethylorthosilicate (TEOS), triton X-100, tris(2,2′-bipyridyl)dichlororuthenium(II) hexahydrate (RuBpy), succinic anhydride, morpholineethanesulfonic acid (MES), bovine serum albumin (BSA), 1-ethyl-3-(3-dimethylaminopropyl)carbodiimide hydrochloride (EDC), and *N*-hydroxysuccinimide (NHS) were purchased from Sigma–Aldrich Chemical Co. Inc. Polycarbonate membranes (hydrophilic, 0.05, 0.2, 0.4, 0.8 μm), ammonium hydroxide (28–30 wt %), and all other analytical reagent grade chemicals were obtained from Fisher Scientific Co. Monoclonal antibodies against *E. coli* O157:H7 were purchased from Biodesign International. *E. coli* O157:H7 and *E. coli* DH5α were obtained from American Type Culture Collections (ATCC). Distilled, deionized water (Easy Pure LF, Barnstead Co.) was used in the preparation of all aqueous solutions.

Design of the Lab-Made Flow Channel Detection System

Figure 1 shows the schematic diagram of our lab-made flow cytometer. An air-cooled Ar^+ laser was used as the excitation source (488 nm, 50 mW). The laser beam was focused on the central region of the micrometer-sized flow channel to probe the bacterial species conjugated with the NPs. The luminescence emission was collected by a high numerical aperture (NA) microscope objective (40X, NA 0.65) placed at 90° to the excitation and sample flow axes. The transmitted light was passed through a long pass (LP 495 nm) filter to reduce the scattered excitation beam. Luminescence bursts were detected with highly sensitive photomultiplier tubes (PMT) (Hamamatsu) with a built-in amplifier system. appropriate optical filter systems were incorporated in front of each PMT to eliminate Raman and Rayleigh scattering, which may interfere with the detection signal. The bursts of luminescence from each bacterium-containing sample were recorded through a 12-bit data acquisition card (NIDAQPad-6020E) interfaced with a computer at a data collection rate of 10 kHz and were then analyzed with custom-built software (LabVIEW). Measurement parameters were optimized before each sample analysis to prevent the output signal level from reaching the threshold level of the acquisition board. The optical detection arrangement can be used for detecting two different bacteria species simultaneously by using two different dye-doped silica nanoparticle–antibody conjugates. For the model design, two different optical filters, long pass filters LP 570 nm and LP 650 nm (labeled F2 and F3, respectively, in Figure 1), were positioned in front of each PMT to ensure that the corresponding emission wavelengths were detected. The optical arrangement can be modified for the detection of three or more different types of bacteria simultaneously.

The sample cell and the flow channel in the optical flow cytometer was a silica microcapillary purchased from Polymicro Technologies (Phoenix, AZ). The inner and outer diameters of the tube were 51 and 358 μm, respectively. An excitation and collection window ($\approx$2 mm in length) was made by burning off the protective polymide sheath of the tube. The microcapillary was then fixed on an XYZ translator stage (Newport). Samples were pumped through the capillary by using a 1-mL syringe (Becton Dickinson, NJ) and a mechanical microliter syringe pump (KdScientific). This setup provided a steady flow of sample through the channel at different flow rates from 1 $\mu L\,h^{-1}$ to 2 $mL\,h^{-1}$.

Synthesis of Dye-Doped Silica Nanoparticles

The reverse microemulsion method (also known as water-in-oil microemulsion) was used to prepare 60 ± 4-nm-sized spherical RuBpy-doped silica NPs, which were characterized with respect to uniformity and luminescence properties.[20] With a water/surfactant molar ratio (W_0) of 10, the reverse microemulsion was prepared by mixing cyclohexane (7.5 mL), *n*-hexanol (1.8 mL), triton X-100 (1.77 mL), RuBpy (0.01 M, 80 μL), and water (400 μL), followed by continuous stirring for 20 min at room temperature. Solutions of TEOS (99.99 % purity; 100 μL) and NH_4OH (29 wt %; 60 μL) were added to initiate the polymerization of $Si(OH)_4$ generated from the hydrolysis of TEOS, and the reaction was allowed to proceed with continuous stirring for 24 h. Carboxylated siliane (25 μL) and *N*-(trimethoxysilylpropyl)ethylenediamine (10 μL) were added to the microemulsion to coat the silica NPs. Finally, carboxylated silica NPs were formed. The NPs were released from the micelles with acetone and thoroughly washed with 95 % ethanol. Ultrasonication and vortexing were used frequently during the washing steps to remove physically adsorbed residual reagents from the NP surface. The dye-doped NPs were air dried and then stored at room temperature.

Immobilization of the Monoclonal Antibodies onto Silica Nanoparticle Surface

To immobilize monoclonal antibodies covalently onto the NP surfaces, the silica surfaces of the RuBpy-doped NPs were first activated with EDC (100 $mg\,mL^{-1}$) and NHS (100 $mg\,mL^{-1}$) in MES buffer (pH 6.8) for 25 min at room temperature with continuous stirring. Water-washed particles were dispersed in PBS (pH 7.3; 0.1 M) and treated with monoclonal antibodies against *E. coli* O157:H7 for 3 h at room temperature with continuous stirring. To reduce the effects of nonspecific binding, the antibody-conjugated NPs were washed in (pH 7.3; 0.1 M PBS) and treated with BSA (1 %) before being used in the immunoassay. With storage at 4 °C, the chemically modified RuBpy-doped silica-coated NPs were viable for several months, while the reporter antibodies were active for up to 2 weeks. If the NP–antibody conjugates are stored at −20 °C, they are also stable for several months.

Detection of the Bacteria

A bacterial sample (500 μL) was dispersed into antibody-conjugated NPs (0.1 $mg\,mL^{-1}$; 500 μL) in a PBS buffer (pH 7.3; 0.1 M) and allowed to react for about 10 min. To remove the free antibody-conjugated NPs that

did not bind to the bacteria, the samples were centrifuged at 14000 rpm for 30 s, and the supernatant was removed. The samples were washed again to remove all unbound antibody-conjugated NPs, and PBS buffer (1.0 mL) was added to the samples. The samples were pumped through the capillary with a 1-mL syringe and a mechanical microliter syringe pump. This allowed a steady flow of sample through the channel at different controllable flow rates. Experiments were conducted at sample flow rates ranging from 1 $\mu L h^{-1}$ to 2 $mL h^{-1}$. Control samples were obtained by using the same experimental procedures but without the addition of bacteria. In the present experiment, the average fluorescence intensity of the controls was considered as the background. Signals above background plus three times the standard deviation (SD) were considered to be positive signals, and this threshold level was set to discriminate the background noise from the positive signal.

Acknowledgements

We thank Dr. Samuel R. Farrah (Department of Microbiology and Cell Science) and Dr. Shouguang Jin (Department of Microbiology and Genetics) at the University of Florida for providing us with the bacteria samples. This work was partially supported by grants from the NSF and NIH.

[1] I. Abdel-Hamid, D. Ivnitski, P. Atanasov, E. Willkins, *Biosens. Bioelectron.* **1999**, *14*, 309–316.
[2] P. M. Griffin, R. V. Tauxe, *Epidemiol. Rev.* **1991**, *13*, 60–98.
[3] B. A. Del Rosario, L. R. Beuchat, *J. Food Prot.* **1995**, *58*, 105–107.
[4] P. S. Mead, P. M. Griffin, B. Swaminathan, R. V. Tauxe, Centers for Disease Control and Prevention (CDC), **2001**, http://www.cdc.gov/ncidod/dbmd/outbreak/ecoli00 summary.pdf.
[5] E. de Boer, R. R. Beumer, *Int. J. Food Microbiol.* **1999**, *50*, 119–130; E. de Boer, *Int. J. Food Microbiol.* **1998**, *45*, 43–53.
[6] X. Zhao, L. Hilliard, S. Mechery, Y. Wang , R. Bagwe, S. Jin, W. Tan, *Proc. Natl. Acad. Sci. USA* **2004**, *101*, 15027–15032.
[7] D. W. Williams, M. A. O Lewis, *Oral Dis.* **2000**, *6*, 3–11.
[8] D. Marie, C. P. D. Brussaard, R. Thyrhaug, G. Bratbak, D. Vaulot, *Appl. Environ. Microbiol.* **1999**, *65*, 45–52.
[9] F. Boisen, N. Skovgaard, S. Ewald, G. Olsson, G. Wirtanen, *J. Assoc. Off. Anal. Chem.* **1992**, *75*, 465–473.
[10] D. M. Gibson, P. Coombs, D. W. Pimbley, *J. Assoc. Off. Anal. Chem.* **1992**, *75*, 231–236.
[11] H. M. Shapiro, *Practical Flow Cytometry*, Wiley-Liss, Hoboken, **2003**.
[12] K. H. Seo, R. E. Brackett, J. F. Frank, S. Hilliard, *J. Food Prot.* **1998**, *61*, 812–816.
[13] S. Santra, P. Zhang, K. Wang, R. Tapec, W. Tan, *Anal. Chem.* **2001**, *73*, 4988–4993.
[14] X. Zhao, T. R. Dytocio, W. Tan, *J. Am. Chem. Soc.* **2003**, *125*, 11474–11475.
[15] M. Bruchez, M. Moronne, P. Gin, S. Weiss, A. P. Alivisatos, *Science* **1998**, *281*, 2013–2016.
[16] W. C. Chan, S. Nie, *Science* **1998**, *281*, 2016–2018.
[17] I. Sondi, O. Siiman, S. Koester, E. Matijevic, *Langmuir* **2000**, *16*, 3107–3118.
[18] a) W. Tan, K. Wang, X. He, X. Zhao, T. Drake, L. Wang, R. Bagwe, *Med. Res. Rev.* **2004**, *24*, 621–638; b) X. Zhao, R. Bagwe, W. Tan, *Adv. Mater.* **2004**, *16*, 173–176.
[19] S. Santra, K. Wang, R. Tapec, W. Tan, *J. Biomed. Opt.* **2001**, *6*, 160–166.
[20] R. Bagwe, C. Yang, L. Hilliard, W. Tan, *Langmuir* **2004**, *20*, 8336–8342; R. Bagwe, L. Hilliard, W. Tan, *Langmuir* **2006**, *22*, 4357–4362.
[21] T. Soukka, H. Härmä, J. Paukkunen, T. Lövgren, *Anal. Chem.* **2001**, *73*, 2254–2260.
[22] R. F. Boyd, *General Microbiology, 2nd ed.*, Times Mirror/Mosby College Publishing, St. Louis, **1988**, pp. 401–404.
[23] E. K. Hill, A. J. de Mello, *Analyst* **2000**, *125*, 1033–1036.

Received: January 20, 2006
Published online: July 18, 2006

